Experimental Study of Systems and Oils for Direct Cooling of Electrical Machine

Ralph Sindjui, Gianluca Zito, Shimin Zhang

Experimental study of systems and oils for direct cooling of electrical machine

Ralph Sindjui[1]

IFP Energies nouvelles ; Institut Carnot IFPEN Transports Energie

1 et 4 avenue de Bois-Préau, 92852 Rueil-Malmaison, France

ralph.sindjui@ifpen.fr

Gianluca Zito

IFP Energies nouvelles ; Institut Carnot IFPEN Transports Energie

1 et 4 avenue de Bois-Préau, 92852 Rueil-Malmaison, France

gianluca.zito@ifpen.fr

Shimin Zhang

Total

Chemin du Canal, 69360 Solaize, France

shimin.zhang@total.com

[1] Corresponding author. IFP Energies nouvelles, 1 et 4 avenue de Bois-Préau, 92852 Rueil-Malmaison, France ; Institut Carnot IFPEN Transports Energie ; ralph.sindjui@ifpen.fr (R. Sindjui)

ABSTRACT

This study presents a test campaign carried out at IFPEN aimed at understanding and characterizing the thermal behaviour of electric motors incorporating direct oil cooling. Several cooling systems and oils are evaluated at different operating points and the effect of parameter variations is investigated. Experimentations are defined and performed to understand and quantify the impact of different oils and direct cooling systems on the performances of the electrical machine. The test results make it possible to verify and quantify the gain on the thermal behaviour obtained by adding an oil injection system directly to the active parts of the machine in addition of an indirect water jacket cooling. This gain is observed for a representative set of operating points and oil injection parameters. The impact of physico-chemical properties of oils on direct cooling performance is assessed by comparison of several oils. The viscous friction losses are also identified. The results presented include a repeatability and reproducibility study for speed values up to 14 krpm and continuous powers up to 60 kW.

Keywords: Electric motors, Oil cooling, Cooling systems, Experimental bench.

1. Introduction

The work presented in this document has been carried out as part of a research project aimed at developing specific experimental means for evaluating cooling systems for electrical machines. For this purpose, an electric motor has been designed in order to be compatible with different oil injection architectures and tested on a test bench. This set-up, combined with the specific instrumentation implemented, allows the analysis of the thermal behaviour for motor speeds up to 14 000 rpm and a continuous power up to 80 kW. Various measurement campaigns were carried out in order to provide: a detailed understanding of the thermal functioning (fluids flow and temperature) of most common

cooling architectures proposed in the literature [1-3]; the identification of design and operating parameters that impact the performance of the cooling system; and finally, the impact of oil properties on the thermal stabilization of the machine. Indeed, understanding these different elements is necessary for the design of efficient cooling systems and the appropriate formulation of fluids in order to improve temperature management in electric machines based on the targeted application [4-6].

Because of climate change, transport vehicle manufacturers are prepared to transition to more sustainable, more efficient and cleaner mobility to reduce the impact of transport on the environment. This environmental emergency is driving governments to take actions through increasingly stringent standards to reduce CO2 emissions and through ecological regulation systems [7]. A new approach to the design of traction systems and a change in vehicles are therefore inevitable. In recent years, the development of electric mobility has been seriously studied in this sector, thus pushing the electric machine design to the fore.

An electrical machine acts as a power transformer, which converts electrical power into mechanical power. In practice, this conversion is not perfect and gives rise to losses in the form of heat dissipation [8]. This can cause serious problems especially if the materials of the active parts of the machine surpass their thermal limits. In fact, beyond a given temperature, these materials lose their properties and the consequences can range from loss of performance to irreversible degradation of the machine [9, 10]. This therefore imposes limitations on the maximum rated performances of an electrical machine, hence the need for efficient cooling systems. Furthermore, because of the

strong requirements imposed by car manufacturers, the trend is to design more and more compact and lighter engines, while seeking a higher power density. This increases even more the challenges of heat dissipation and the design of more efficient cooling systems.

Conventional cooling consists in cooling the casing of the machine which surrounds the stator. However, in such a system, the heat generated at the heart of the machine must pass through areas and interfaces where the thermal conduction is not ideal. Direct cooling of the hot parts is therefore more efficient, by using a heat transfer fluid as an exchanger to dissipate the heat generated during the operation of the machine. The work presented in this article therefore focuses on the experimental study of systems and fluids for direct oil cooling of electric motors for traction.

The paper is organized as follows: first the experimental setup used for the study is presented detailing the different types of cooling systems and the different parameters of oils used. Then the methodology for calculating heat exchanges as well as the various tests carried out are also detailed in section 2. Section 3 presents the analysis of viscous friction losses of the machine and the comparisons made for different architectures and different oils. Thereafter, the analysis of heat exchanges is addressed for each configuration, as well as the analysis of the thermal behaviour of the machine for each type of cooling. Finally, a discussion of the experimental methods used, the perspectives for the study and a summary of the experimental results are presented.

2. Experimental setup

The first step in carrying out this study is the manufacturing of a machine prototype allowing the integration of different cooling architectures and the set-up of a

test bench capable of accommodating several types of oils. Cooling architectures selected from the literature present the best compromise in terms of performances and complexity of implementation [1-3]: these architectures are studied upstream of the campaign to allow comparison with the same cooling parameters (temperature, flow) and the same machine. In addition, the aim of the study being to estimate the heat exchanges, the design of the engine cooling zones is driven by this objective and well thought out in order to allow better modelling of the heat flows. In the same way, the instrumentation has been judiciously defined. Moreover, in order to study the thermal stabilization of the machine over a wide operating range, a high-power application has been considered to be representative of traction electric motors.

According to these specifications, a prototype has been designed and manufactured and a test bench is implemented for the needs of the study.

2.1. System presentation

2.1.1. Principle

The designed machine has a peak torque of 260 Nm for a peak current of 640 A, a mechanical peak power of 150 kW, a peak efficiency of 96 % and a maximum operative speed of 14 000 rpm. In continuous performance (with a standard water jacket cooling), it allows operation at a continuous torque of 130 Nm at 6000 rpm corresponding to a continuous mechanical power of 80 kW. The motor is supplied by a prototype inverter with a nominal DC voltage of 350 V. Its mechanical performance curve is presented in Figure 1.

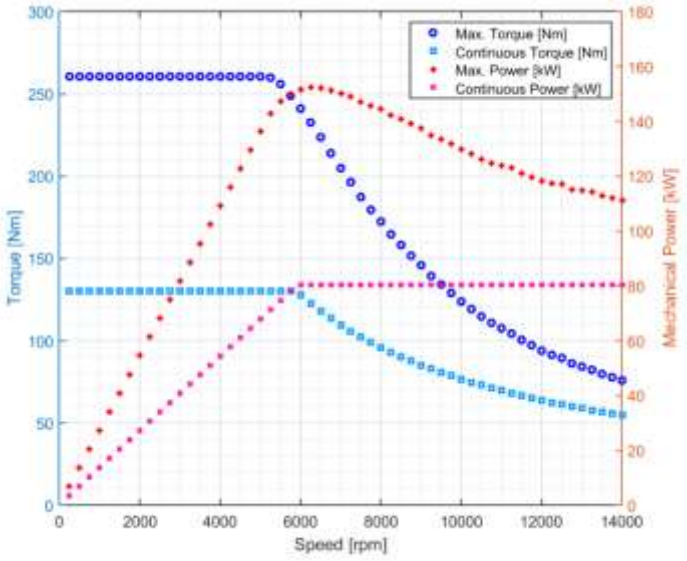

Figure 1 Mechanical performance of the machine manufactured for the study

This machine is designed with a casing incorporating a conventional water jacket surrounding the stator, and an additional water-cooling circuit in each flange closing the machine for thermal measurement purpose. Thanks to the water-cooling systems, it is possible to impose a thermal envelope around the electrical machine for an optimal quantification of the heat exchanges. The objective of the design being the study of active direct oil cooling (projection of the fluid on the windings), two fluid distributors are provided between the winding and each flange. These modular distributors allow the integration of different oil injection architectures. Oil extraction systems are also integrated at the bottom of the casing. The principle of the general cooling architecture implemented is illustrated in Figure 2.

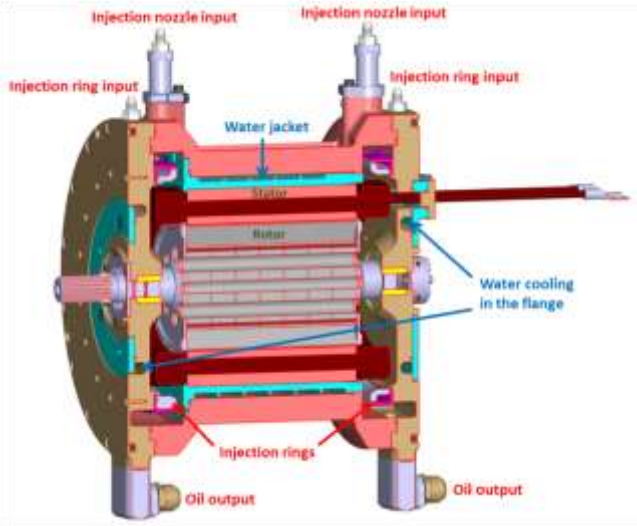

Figure 2 General architecture implemented for the study on direct oil cooling

The stator winding is instrumented with temperature sensors. Five measurement points (see Figure 3) are accessible via thermocouples directly integrated into the coils : a sensor on the coil heads on the phase output side (A), a sensor in the centre of the stator (B), a sensor on the coil heads on the opposite side at the phase output (C), a sensor in the upper of the slot on the phase output side (D), and a sensor at the bottom of the slot on the phase output side (E).

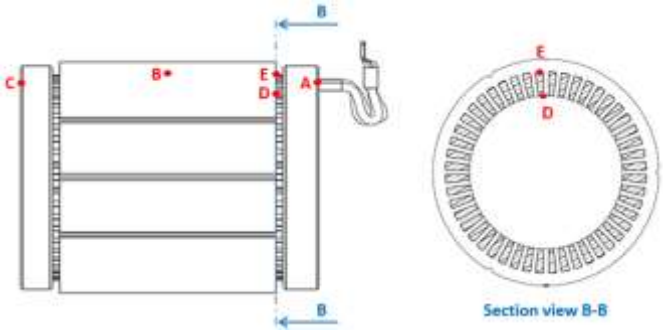

Figure 3 Stator instrumentation

The water and oil circuits are also instrumented with pressure, flow and temperature (thermistor) sensors to monitor the pressure at the outlet of the supply

group, the flow in each branch of the cooling circuit as well as the temperature at the inlet and outlet. The sensors used have accuracies of ± 0.1°C, ± 1°C and ± 6 l/h, for thermistors, thermocouples and flow measurements respectively.

Additional sensors are added to the machine housing and the bench to allow modelling of heat exchanges by conduction and convection (between the machine and the bench environment). In order to quantify this thermal flow, preliminary tests are carried out in a temperature range between 25 °C and 80 °C to identify the thermal inertia. This allows to estimate the convective exchange coefficient between the electric machine and the bench cell. This exchange coefficient is necessary for the estimation of the flows exchanged with air. These tests highlight the need to thermally isolate the machine and the circuit. Indeed, without thermal insulation, the water circuit heats the casing and a large flow is dissipated in the air. This phenomenon would be problematic for an accurate estimation of the thermal flows as the water cooling will extract heat from the dissipative parts of the machine and part of this heat will be lost in the air and cannot be quantified. Figure 4 illustrates the electric motor prototype before and after the thermal insulation. It has been estimated that the insulation reduces the equivalent heat exchange coefficient by a factor of two compared to a configuration without insulation. In addition, it leads to a reduction in the variation of the heat flux dissipated by the water over the entire temperature range and thus an accurate estimation of thermal balances.

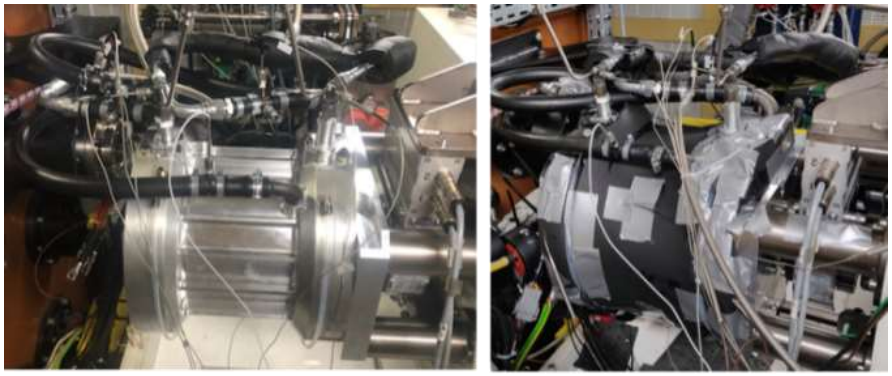

Figure 4 Prototype and instrumentation before (left) and after (right) the thermal insulation

2.1.2. Injection systems

In order to test the thermal sensitivity linked to the cooling architecture, two main architectures have been selected for this study:

- The first one enables to test injection nozzles [11-14] above the end-windings and a gravity flow around their periphery. For this architecture, two types of commercial injectors are used and allow working in a flow range from 120 to 480 l/h. One configuration is a flat jet nozzle allowing a large projection angle, the winding is therefore impacted over a large but not very wide angular range. The other one is a full cone nozzle which consists in impinging the upper part of the winding more widely. The rest of the winding is cooled by the gravity flow of the oil to the bottom of the casing.
- In the second architecture, a ring is placed around the end-winding with a distribution of orifices on it. For this architecture, two configurations have been designed, and the admissible flow rate is in the range from 120 to 480 l/h: a configuration in multi-

jet type with sixteen outlet holes over the entire circumference; a configuration in dripping type containing five outlet holes positioned on top of end-windings.

Figure 5 presents a summary of the different oil cooling architectures tested.

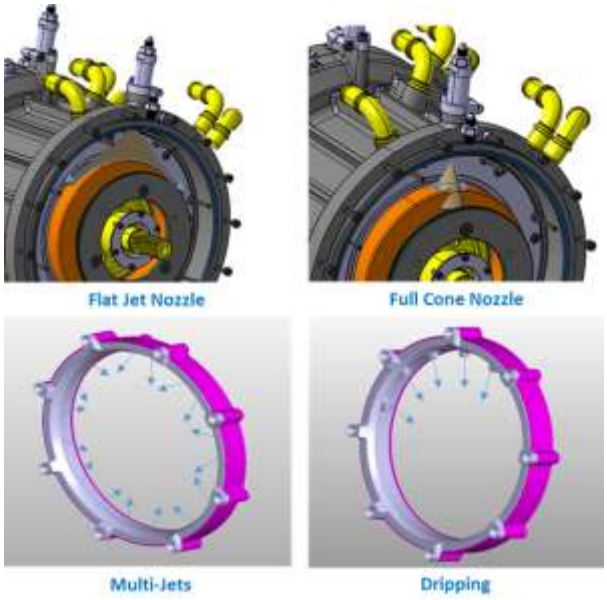

Figure 5 Oil injection architectures integrated in the prototype

2.1.3. Different types of oils

Four fluids (referenced as F1, F2, F3 and F4) that are electrically compatible and have different properties are selected and manufactured in partnership with Total™ for this study. Their characteristics are listed in Table 1. They are chosen by their chemistry and physicochemical properties in order to understand the impact of oils on cooling, and the interactions between the fluid and other factors, such as cooling architecture, flow rate, temperature.

Reference	Composition			KV 40* [cSt]	KV 100* [cSt]	Purpose
F1	Gr III/PAO	Additive		25.89	5.28	Reference
F2	Gr V	Additive		7.96	2.47	Formula chemistry
F3	Gr III/PAO	Additive		8.73	2.48	Viscosity
F4	Gr III/PAO	Additive	Polymer	11.71	5.24	Viscosity under shear

Table 1 Characteristics of oils selected for the study

**KV40: kinematic viscosity at 40°C; *KV100: kinematic viscosity at 100°C*

The cooling performance of fluid could be assessed by a physically based *Figure of Merit* (*FOM*) [15]. In the case of direct cooling by a laminar flow, the *FOM* on average heat transfer F_h is expressed as

$$F_h = \frac{\rho^a Cp^b k^c}{v^d} \quad (1)$$

where *ρ* is the density, *Cp* the heat capacity, *k* the thermal conductivity and *v* the kinematic viscosity; *a-d* are parameters depended on the contact geometry.

These four fluids are different in their formulation. The most important difference between these fluids is their kinematic viscosity. At 40 °C, the fluid F1 has a viscosity three times higher than F2 and F3. The other properties have a slight difference of between 5 % and 7 %, over the entire temperature range. Fluid F4 has a reduced viscosity with shear due to the presence of polymers in its formulation. As the shear rate changes with the size of the injector, this fluid could have interesting behaviour for some injection architectures.

F1 has been studied as a reference for the comparison between different injection architectures, and the other three fluids are studied in the context of the comparison of fluids. For this reason, their comparison will not be presented (in this document) for all architectures. However, the verification of trends was indeed carried out as part of the study. The physicochemical properties are also illustrated in Figure 6.

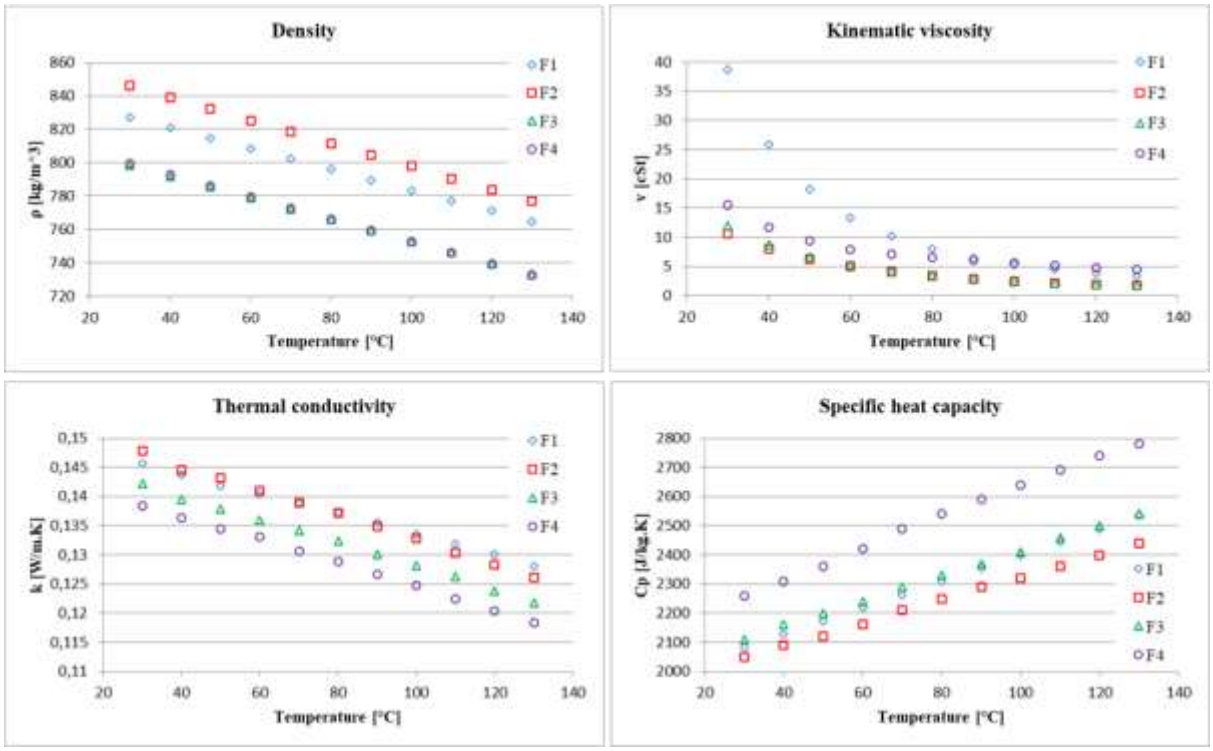

Figure 6 Illustration of experimental physicochemical properties of oils selected for the study

2.2. Tests

Several types of measurements are performed for this study. Table 2 presents a summary of the different types of tests and parameter (temperature, flow rate, operating point) variations carried out.

Test	Operating point	Water temperature	Water flow rate	Oil temperature	Oil flow rate
Preliminary	0 rpm	From 25 °C to 80 °C	720 l/h	N/C	N/C
No-load	Speed up to 14 000 rpm No load	From 25 °C to 85 °C		From 25 °C to 80 °C	From 120 l/h to 480 l/h
On-load	Speed up to 14 000 rpm Power up to 60 kW	65 °C		From 40 °C to 80 °C	From 240 l/h to 480 l/h

Table 2 Summary of the different types of tests carried out and the different parameters

2.2.1. Preliminary tests

Convective exchanges between the ambient air and the engine have a direct influence on the accuracy of the thermal balances because of the uncertainty of measurement in each test. This is the reason why it is necessary to quantify them, with a dedicated process in order to determine their impact on the thermal balance and consider corrective actions on prototype conditioning if required. Therefore, specific thermal inertia tests have been carried out in order to estimate the convective exchanges between the casing of the electric machine and the ambient air in the cell of the test bench. These tests are performed with the electric machine at rest, activating only the water-cooling circulation (50-50 glycol-water). The details of this phase are discussed in section 2.3.1.

2.2.2. No-load tests

The aim of this type of test is to quantify the impact of fluid's properties and/or of an oil injection architecture on viscous friction losses. The friction losses depend essentially on the speed. However, since the cooling is direct, it is essential to check the influence of the addition of a fluid (including its properties and the injection method used) on the viscous friction of the machine. The test method consists in driving the electric machine by the motor of the test bench by carrying out a sweep over the entire speed range (from 500 rpm to 14 000 rpm in our case). The no-load torque is thus measured on the shaft line at the coupling with the electric machine. The power lost by friction is thus calculated.

In order to define the impact of adding direct oil cooling system, it is necessary to define reference running tests without oil injection. These tests will serve as benchmarks for comparison with different given cooling configurations. In this study, the reference tests are carried out with the presence of water cooling allowing a thermal envelope around the electric machine (water jacket). Oil cooling is then added to water cooling at the same temperature, allowing the estimation of the impact of oil cooling. The viscosity of the oil being strongly dependent on the temperature (as shown on Figure 6), this characterization is performed at different temperatures. Several characteristics are thus obtained as a function of the speed, a curve for each oil temperature. It is also necessary to characterize the impact of the injection flow rate on viscous friction losses. The same approach as that of the temperature is therefore followed within the framework of the characterization for different flow rates.

2.2.3. On-load tests

On-load tests with cooling allow quantification and analysis of the impact of oil cooling on the thermal behaviour of the machine in operation. Initially, reference tests are carried out without oil cooling (cooling by the water jacket only). The same test points are carried out with oil cooling using the different architectures under study. These points with oil cooling are compared to the reference and thus the impact of oil cooling can be quantified. Similarly, to the no-load case, the impact of the flow rate and the temperature of the oil injected is evaluated.

2.3. Methodology

The methodology is detailed for each type of test presented in the previous section 2.2.

2.3.1. Preliminary tests methodology

In this test configuration, the water provides heat which is diffused in the casing of the machine and is transferred by convection into the ambient air and by conduction towards the test bench. A heat balance is carried out using the stabilized values of the measurements in order to quantify the heat fluxes provided by the water and received by the ambient air, as well as the conductive losses towards the bench.

The thermal power provided by the water P_{water} is calculated by

$$P_{water} = \dot{m}_{water} c_{p_{water}} \left(T_{water_{out}} - T_{water_{in}}\right) \quad (2)$$

where $\dot{m}$ is the mass flow, c_p the heat capacity, $T_{water_{out}}$ the outlet temperature and $T_{water_{in}}$ the inlet temperature of the coolant.

The thermal power transferred by conduction to the test bench P_{bench} is considered in order to refine the thermal balance. This power can be estimated by

$$P_{bench} = \frac{\Delta T_{M-bench}}{R_{th}} \quad (3)$$

where R_{th} is the thermal resistance calculated for the four columns used to support the machine (see Figure *4*) and which thus thermally connect the electric machine to the bench, $\Delta T_{M-bench}$ is the temperature gradient measured between the machine housing and its supports [16, 17].

The power exchanged with the ambient air P_{air} is given by

$$P_{air} = \alpha_{HTC_{air}} S_e (T_{hous} - T_{air}) \quad (4)$$

where $\alpha_{HTC_{air}}$ is the convective air exchange coefficient, S_e the exchange surface between the machine and the ambient air, T_{hous} the machine housing temperature and T_{air} the ambient air temperature.

A first balance of powers P_{tot} is thus obtained allowing the estimation of the convective transfer coefficient between the machine and the test bench

$$P_{water} + P_{air} + P_{bench} = P_{tot} \approx 0 \quad (5)$$

2.3.2. No-load tests methodology

The power lost by friction is the product of the measured friction torque at no-load and the motor speed. Since the initial conditions of the machine have an impact on loss measurement, the sequence of tests should be properly defined in order to avoid measurement errors. In this study, a rest time is left between each no-load test until the measured temperatures return to the same initial condition. Each test is repeated several times in order to estimate the dispersion of the measurements. This allows to quantify the random errors. The comparison between the different cooling parameters is then performed on the arithmetic means of the associated series of observations. For comparison, each point is illustrated with an error bar representing the maximum standard deviation associated with each series. For better readability, error bars are not displayed when two curves overlap.

2.3.3. On-load tests methodology

For each test point, a thermal balance is carried out and the different thermal powers are calculated/estimated from the measurements obtained in steady state. The total thermal power obtained is compared to the measured total losses of the machine ($P_{total-loss}$) in order to quantify the quality of the test considered. The total losses of the machine are obtained by difference between the three-phase electrical power measured at the input and the mechanical power measured at the output.

In addition, the temperatures measured by the sensors integrated in different places of the stator (see section 2.1.1) are compared in order to quantify the performance

of oil cooling and to compare the impact of the cooling architectures on the temperature distribution (winding and stator stacks).

The different thermal powers are calculated as detailed in section 2.3.1. When oil cooling is used, the heat power absorbed by the fluid P_{oil} is calculated by

$$P_{oil} = \dot{m}_{oil} c_{p_{oil}} \left(T_{oil_{out}} - T_{oil_{in}} \right) \quad (6)$$

This heat absorbed by the oil circuit is added to the heat balance written in relation (5) to give the overall thermal power $P_{thermal}$ of the system (including the oil circuit). The contribution of each cooling circuit to the heat exchange is obtained by means of the corresponding heat flows. Thus, we can quantify the accuracy of each test through the following parameter ε :

$$\varepsilon = \frac{P_{thermal} - P_{total-loss}}{P_{total-loss}} \quad (7)$$

3. Friction losses analysis

To assess the impact of oil injection on viscous friction losses, tests are first carried out without oil as described in section 2.2.2. Figure *7* shows the no-load losses obtained for a variation in glycol-water temperature ranging from 25 °C to 85 °C and for a constant flow rate of 720 l/h.

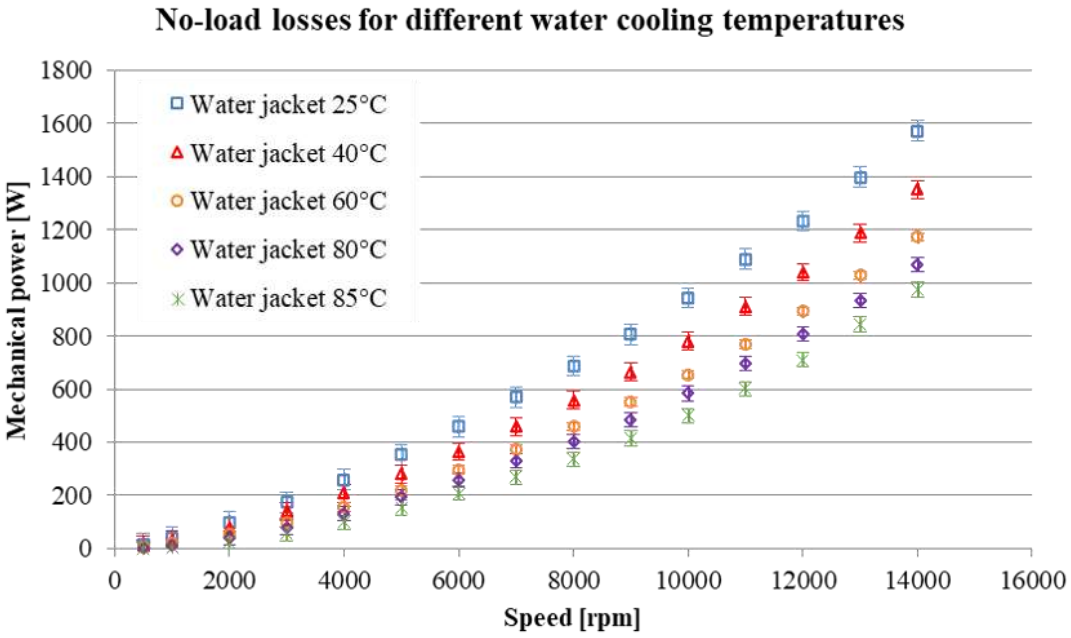

Figure 7 No-load losses for different water-cooling temperatures

For a given cooling temperature, the mechanical power at no-load can be approximated by a quadratic form [18] depending on the driving speed of the machine. Moreover, it decreases when the cooling temperature increases. For a speed of 14 000 rpm, a decrease in the mechanical no-load power of about 600 W is observed for an increase in water cooling from 25 °C to 85 °C. This decrease can be explained by the reduction in mechanical losses in the bearings and seals with the increase in temperature [18]. In addition, when the temperature increases, the magnetic flux induced by the magnets decreases and leads to a decrease in iron losses [10].

The oil circuit is then activated in addition to the water circuit and parametric variations are made for each architecture and for each oil, under the conditions described in section 2.2.2. For all these measurement conditions (temperature variations and oil

flow ranges considered presented in Table *2*), there is no significant impact of the addition of direct oil cooling on the no-load losses, in comparison with the reference tests.

The variation of oil flow also has a low impact on viscous friction losses for the different oils and injection architectures. The temperature variation of the water and oil follows the trend presented in Figure *7*. Concerning the variation in flow, an example is given in Figure *8* which presents the variation from 120 l/h to 480 l/h with a flat jet nozzle (see Figure 5), for a given cooling temperature of 60 °C (water and oil). The reference test is also shown on the same graph to illustrate the impact of the oil presented above. These trends are observed for the entire measurement range presented in Table *2*.

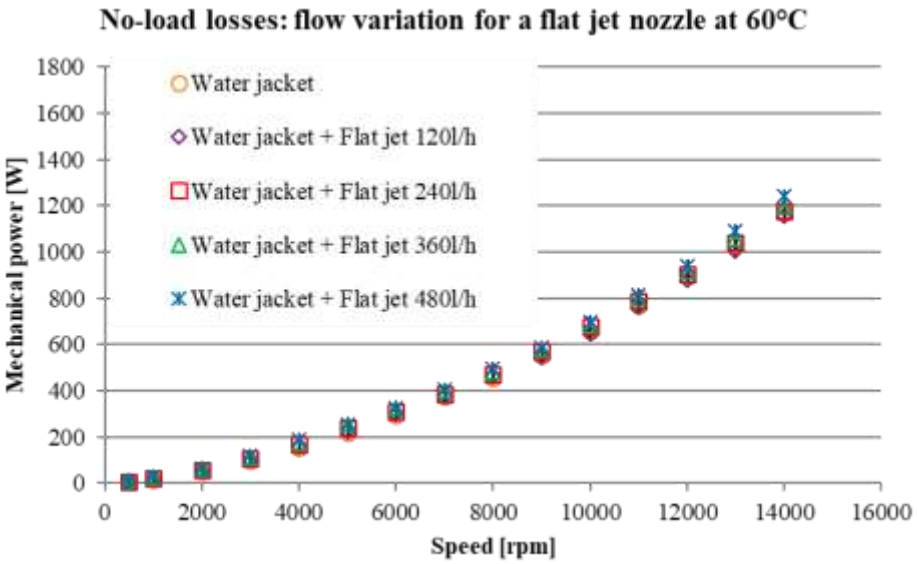

Figure 8 No-load losses for different flow rates for a flat jet nozzle and a given cooling temperature of 60 °C (water and oil)

3.1. Friction losses analysis: Architectures comparison

Similarly, no significant impact of the cooling architectures on the viscous friction losses of the electric machine has been observed. As an example, the Figure *9* presents the comparison of the losses observed for a given flow rate of 360 l/h and a temperature of 60 °C for the four architectures presented in Figure 5.

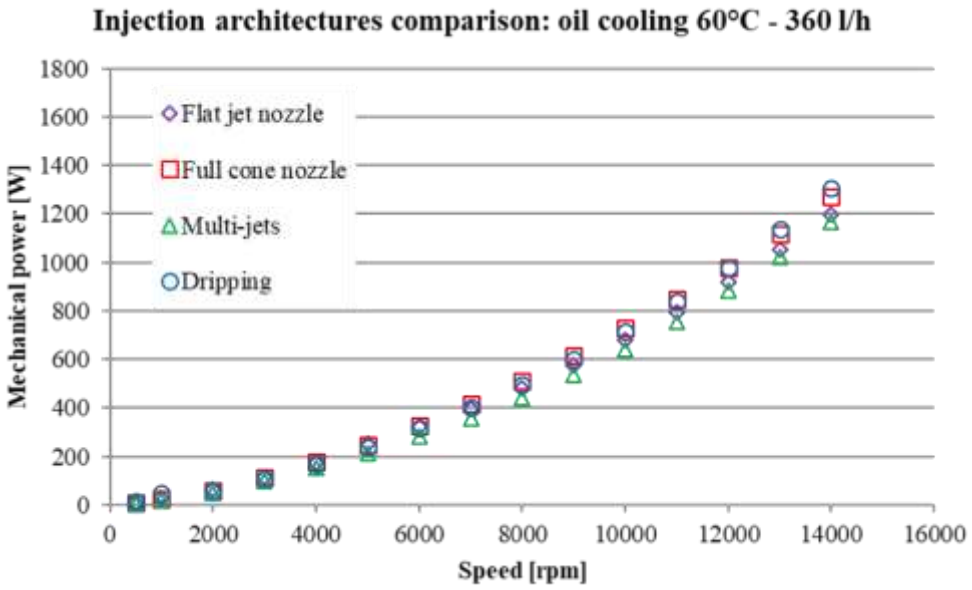

Figure 9 No-load losses: injection architectures comparison for a given cooling temperature of 60 °C (water and oil) and an oil flow rate of 360 l/h

3.2. Friction losses analysis: Oils comparison

The main observation made for the comparison of fluids is that the viscous friction losses are mainly related to the viscosity of the fluid in contact with the shaft line [18]. In fact, lower viscosity implies lower losses. Concerning the fluids of this study, the comparison is therefore more effective at low temperature (40 °C) because it allows to

discriminate the kinematic viscosity of the fluids (see Figure 6). Moreover, the higher the temperature of the fluid is, the lower the losses will be (as presented on Figure *7*) and therefore more difficult to discriminate different fluids. It is important to mention, however, that the observed variation in no-load losses with viscosity is small and is around 100 W (at the most) on all four fluids.

4. Heat exchange analysis

Using the methodology presented in part 2.3 and the instrumentation in place, the flux captured by each branch of the circuit is calculated. This provides an overview of all heat exchanges at the engine level. The tests carried out for the identification of flows are those described in section 2.3.3. Tests are carried out over a period of 90 minutes to have a consistent thermal stabilization. A maceration time of around 60 minutes is also systematically left before the start of each test. The flow calculations are performed on temperature values averaged over the steady state (which corresponds to an averaging over 30 minutes minimum). As for the no-load losses test series, first reference tests with glycol-water cooling were carried out (for fixed temperatures and flow rates of 65 °C and 720 l/h, respectively) before adding the different oil cooling configurations for comparison.

The power captured by the oil linearly decreases with increasing oil temperature as illustrated in the Figure *10*. This strong linear correlation is identified on the thermal behaviour of the stator sensors. It can be observed that the temperature gain decreases drastically when the temperature of the cooling oil is increased (this trend is detailed in section 5).

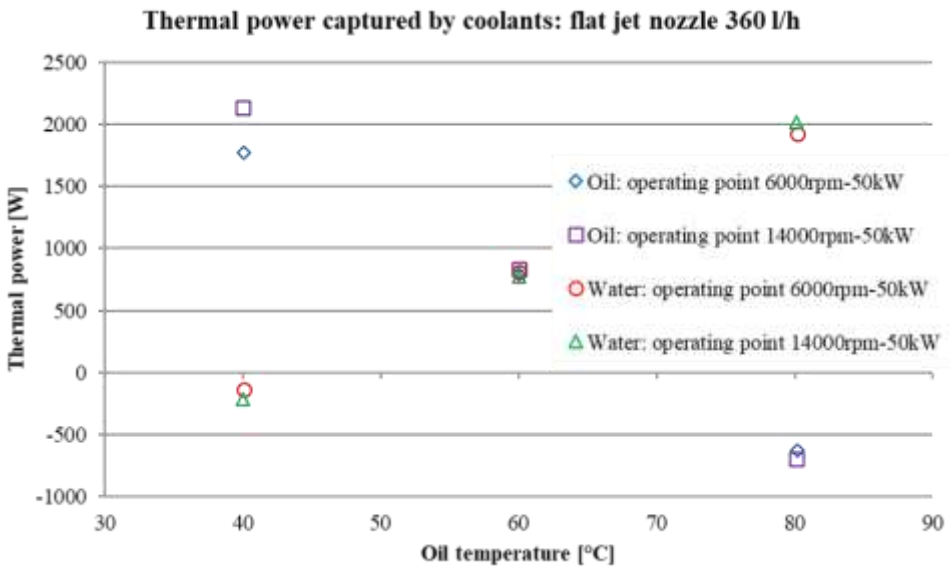

Figure 10 Power captured by the coolants for a given oil flow rate of 360 l/h: impact of the oil temperature on the thermal power

Moreover, the power captured by the oil increases with the increase in the oil flow (see Figure *11*). There is an increase on the order of 400 W maximum for a fixed temperature of 60 °C and a flow rate ranging from 180 l/h to 480 l/h. This small variation should not affect the overall thermal response of the machine because of the compensation of the water circuit on the heat exchange.

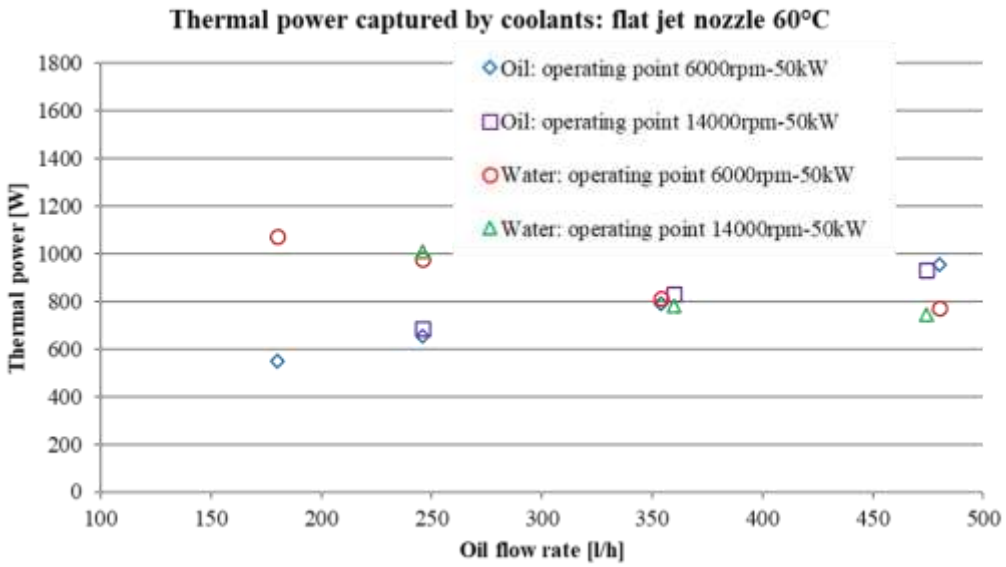

Figure 11 Thermal power captured by the coolants for a given oil temperature of 60 °C: impact of the oil flow rate

4.1. Heat exchange analysis: Architectures comparison

Regarding the influence of the cooling architecture, no significant impact was observed (Figure 12) on the heat flow among the four architectures selected for the study. It is important however to associate this observation with the thermal response of the machine (section 5) to have the thermal contribution of each architecture.

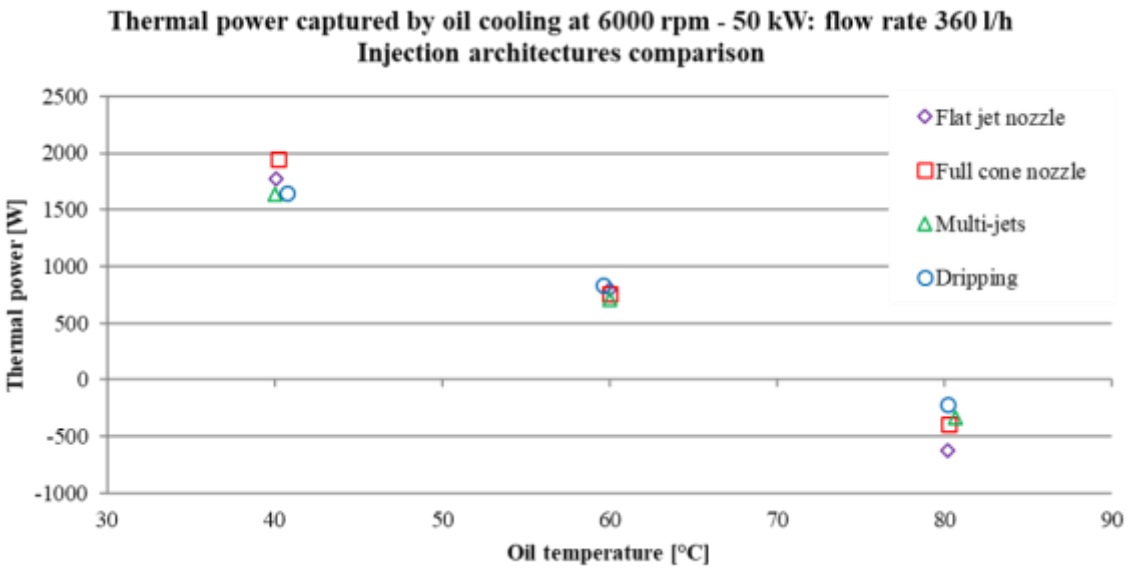

Figure 12 Power absorbed by oil cooling: temperature variation and architecture comparisons for a given flow rate of 360 l/h and an operating point of 6000 rpm - 50 kW

4.2. Heat exchange analysis: Oils comparison

Figure *13* shows the evolution of the power absorbed by the four oil variations versus temperature, for a fixed flow rate of 360 l/h and an operating point of 6000 rpm - 50 kW. The gap in absorbed thermal power between F1, F2, F3 and F4 is the highest at low temperatures (40 °C) and decreases considerably for higher temperatures. This observation is coherent with the trend observed for the kinematic viscosity when comparing different fluids (see Figure 6). For the other properties, the difference is relatively constant with the increase in temperature. We therefore deduce that the power captured by the oil is mainly dependent on its viscosity and the more viscous the fluid, the less the ability to capture heat will be. Both the viscosity and the heat capacity have an impact on the power absorption, while the impact of viscosity is less obvious. The heat transfer between the machine and oil flow is mainly via forced convection. At the jet

impingement zone, the oil flow is partially turbulent. Flow regime is determined by the Reynolds number, which is related to the fluid viscosity. When the fluid has a low viscosity, its flow is prone to turbulence [22, 23], and therefore increase the heat transfer rate. Moreover, the viscosity impacts the thickness of viscous sublayer, which is a laminar layer between the wall and upward turbulent flow. A high viscosity fluid tends to have a thick viscous sublayer, and thus reduce the heat transfer rate. In this work, the fluids have almost similar heat capacity, while their viscosity is more diverse and therefore appear to have a more significant impact on the heat absorption. At 40 °C - 360 l/h for the example shown in Figure *13*, we have a difference of about 600 W for a viscosity difference of about 30 cSt (between F1 and F4).

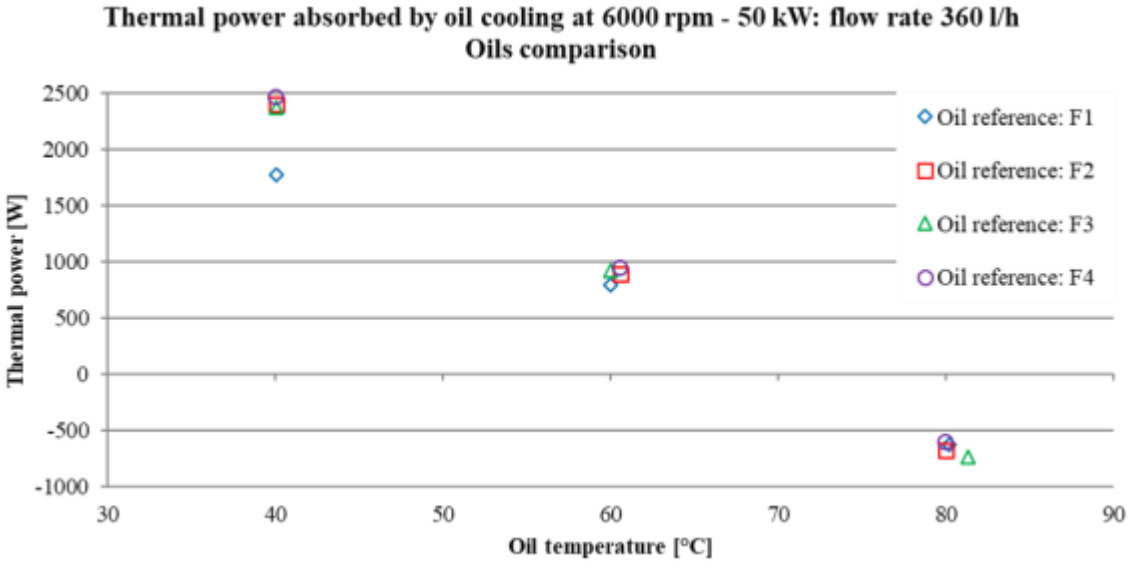

Figure 13 Power absorbed by oil cooling: temperature variation and oil comparisons for a given flow rate of 360 l/h and an operating point of 6000 rpm – 50 kW

5. Analysis of the thermal behaviour of the machine

The tests performed for the heat exchange analysis presented in Section 4 can also be used to study the impact of direct oil cooling on the thermal stabilization of the machine. In this context, the thermal reference (water jacket cooling) is observed at first (see Figure *14*). This first step also allows us to observe the temperature distribution in the stator through the five different thermocouples mounted in the winding at strategic locations (see section 2.1). Thus, the gain in temperature can be evaluated over the entire speed range up to 14 000 rpm and a power range up to 60 kW. As a precaution for the machine, this load has not been exceeded for continuous tests and represents the maximum load up to which the observations are made in this part.

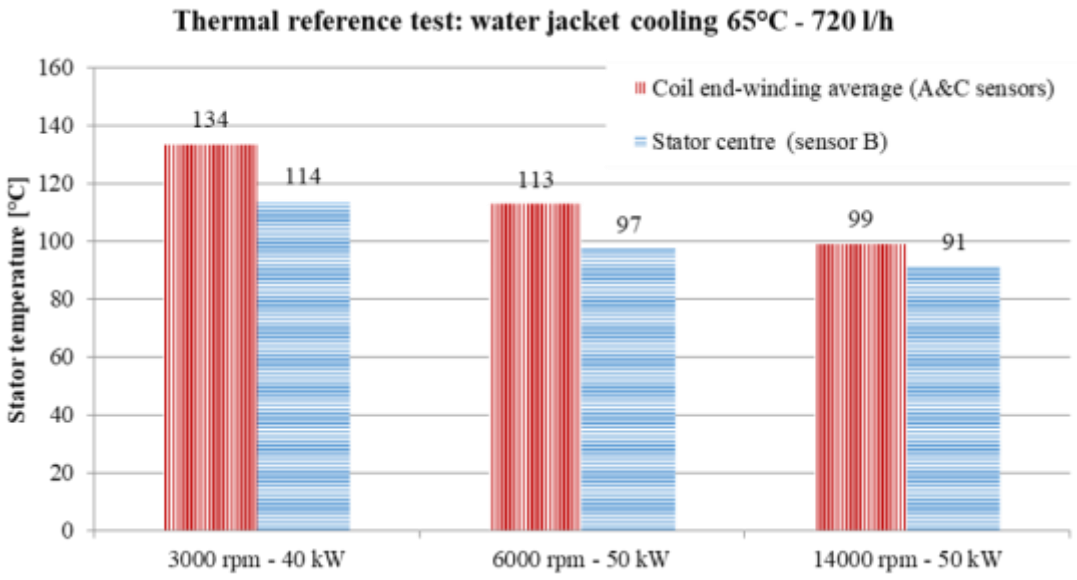

Figure 14 Thermal reference test: water jacket cooling temperature 65 °C and flow rate 720 l/h

Due to the presence of the water chamber around the stator, the centre of the stator (relatively to the active length) is better cooled and the hot spots are located at the coil end-winding. A relative difference of about 20 °C is observed between the centre of the stator and the coil end-winding, for an operating point of 3000 rpm – 40 kW. As expected, the temperature measured on the stator is higher at low speed than at high speed as, for a given power, a higher torque is needed at low speed. As the torque is directly linked to the intensity of the current flowing through the winding, the higher the torque, the higher the current required, therefore implying a more dissipated power by Joule effect. As a result, the stator temperature is generally higher at low engine speeds, which creates a more favourable condition to highlight the impact of an additional coolant fluid.

Unlike to the observation made on thermal flows, the impact of the variation in flow rate is not significant on the thermal response of the electric motor (variation presented on Figure *15* for a flat jet nozzle and an operating point of 6000 rpm – 50 kW). Indeed, the power captured by the oil increases with the increase in the oil flow. However, this phenomenon does not affect the thermal response because the variation in the oil thermal power (as a function of the oil flow) is compensated with the power absorbed by the water circuit. This heat flux decreases linearly with the oil flow, which clearly shows this compensation effect. Moreover, the measured temperature decrease is inversely proportional to the oil temperature and highly dependent on the latter. The geometry of the machine being fixed, the parameter which will mainly impact the heat transfer by convection is the temperature gradient between the oil and the stator. When the oil

temperature increases, this gradient is reduced and therefore the power absorbed by the oil also decreases.

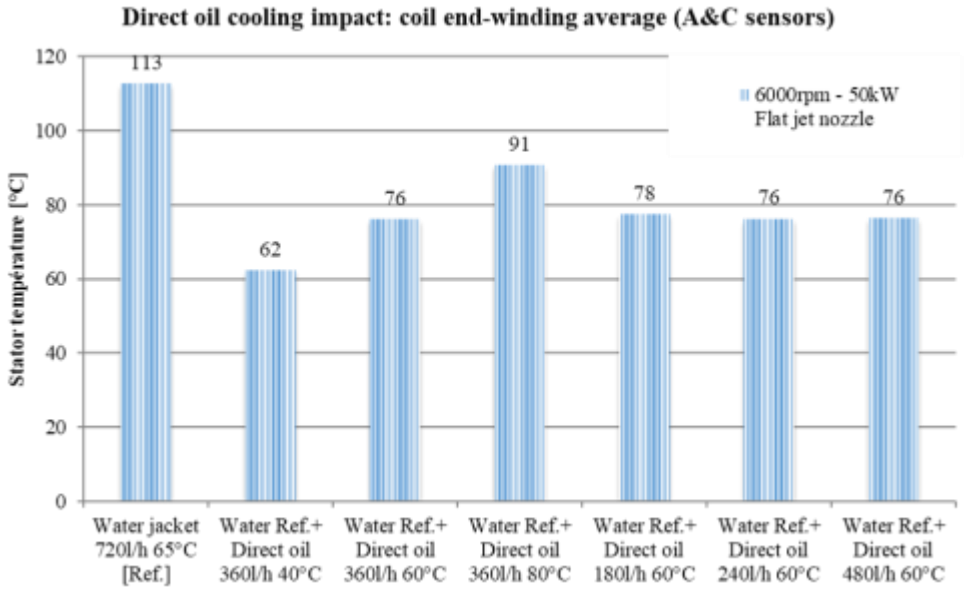

Figure 15 Direct oil F1 cooling impact: coil end-winding average temperature for various oil cooling parameters, flat jet nozzle and operating point of 6000 rpm – 50 kW

A considerable decrease in temperature is observed when coupling standard water jacket cooling with oil injection. As shown in Figure *16*, a gain of around 50 °C is observed on the end-windings for the addition of oil cooling (40 °C – 360 l/h) with a flat jet injector at an operating point of 6000 rpm – 50 kW. The coil end-windings temperature (A&C sensors) decreases from a temperature of 113 °C (for a water reference test at 65 °C) to a temperature of 62 °C (when injecting oil at 40 °C on the coil end-winding). The centre of the stator (sensor B) is also affected, as the oil cools the winding by conduction from the coil end-winding towards the centre: lower but nevertheless notable gains are obtained in the range of 25 °C to 30 °C when injecting oil

at 40 °C and an operating point of 6000 rpm – 50 kW. Consequently, the hot spots are moved to the centre of the stator when injecting oil directly on the coil heads. One can observe that in this case the centre of the stator has a much lower temperature level when compared to the reference test (for example from 97 °C to 72 °C at 6000 rpm and 50 kW).

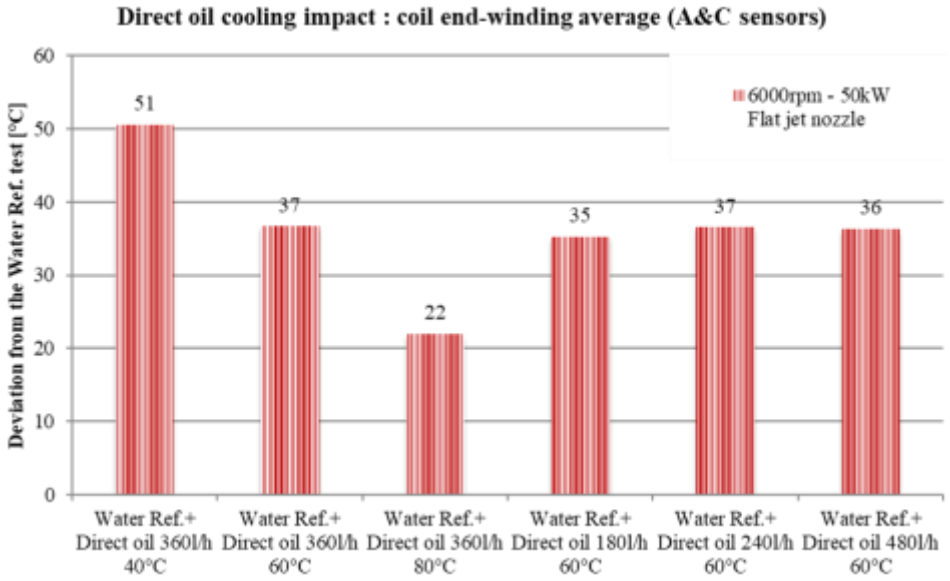

Figure 16 Gain from adding oil F1 with a flat jet injector on the end-windings average temperature, for different oil cooling parameters and an operating point of 6000 rpm – 50 kW

5.1. Thermal performance: Architectures comparison

Figure *17* illustrates the comparison of the temperature gain obtained for the different architectures and for an operating point of 6000 rpm – 50 kW. It appears that jet type and dripping architectures offer similar cooling and that the multi-jet type architecture is slightly less efficient than the other three. However, it is important to

mention that the temperature results presented in this document should be analysed considering the instrumentation of the stator used during the study (five sensors). The use of additional thermal sensors, foreseen in further studies, will allow to refine the analysis and thus give a better visibility on the axisymmetric behaviour of the stator temperatures.

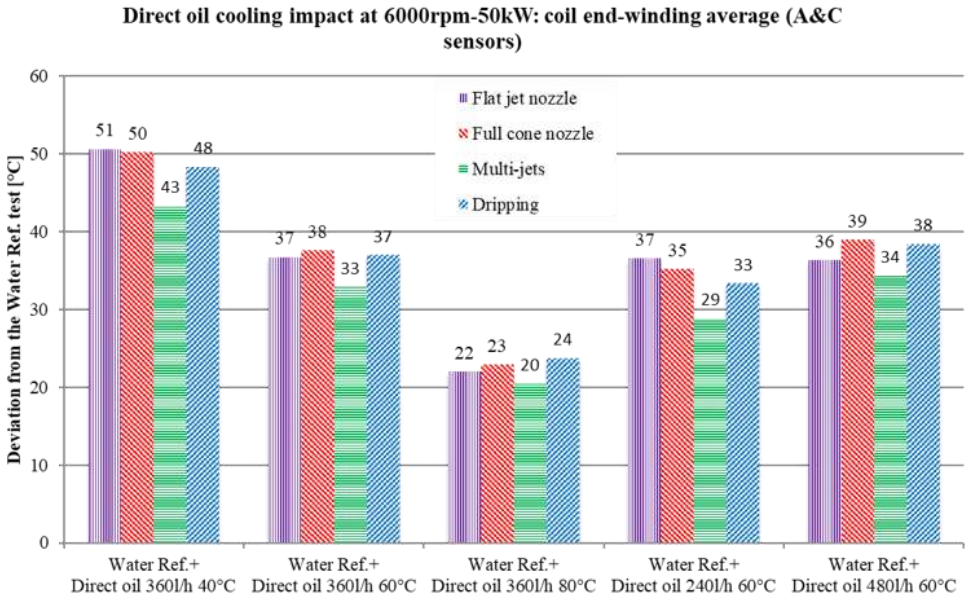

Figure 17 Gain from adding oil F1 for different cooling architectures on the end-windings average temperature, for different oil cooling parameters and an operating point of 6000 rpm – 50 kW

5.2. Thermal performance: Oils comparison

Figure *18* illustrates the comparison of the temperature gain obtained with a flat jet type injection, for the different oils and for an operating point of 6000 rpm – 50 kW. Low viscosity fluids have better cooling power. This observation is more marked when cooling at 40 °C than for higher temperatures. This latter temperature corresponds to the

temperature at which the viscosity discrimination is most obvious (see Figure 6). As the difference in terms of temperature gain between the four fluids remains small, a repeatability study is integrated into the test campaign to check the degree of confidence on the differences obtained. This aspect is commented on in section 6. The impact of injection architectures on the cooling performance is low for fluids of different viscosities.

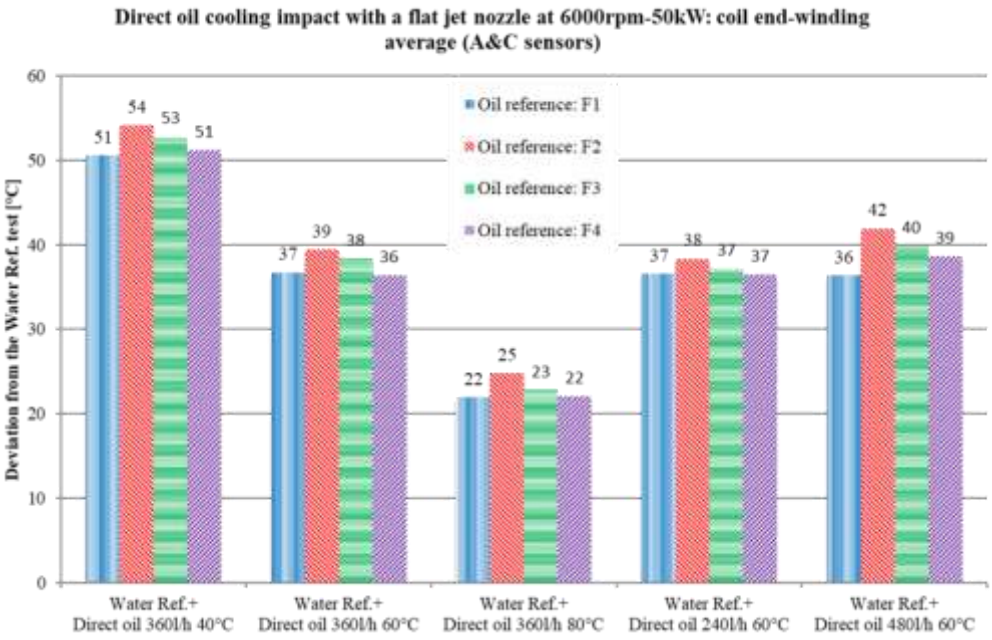

Figure 18 Gain from adding different oils with a flat jet nozzle on the end-windings average temperature, for different oil cooling parameters and an operating point of 6000 rpm – 50 kW

6. Discussion

In order to obtain accurate thermal balances, all the results presented so far are carried out with an active water cooling. However, we observed that under certain conditions, especially for an oil at 40 °C, the thermal power absorbed by the water jacket is negative (see Figure 10). This negative flow means that overall, the water heats the

engine instead of cooling it because the reference temperature is higher (65 °C). These results seem to confirm that the oil alone injected on the coil end-winding is sufficient to properly cool the machine, and that it is possible to carry out tests without a water-cooling circuit.

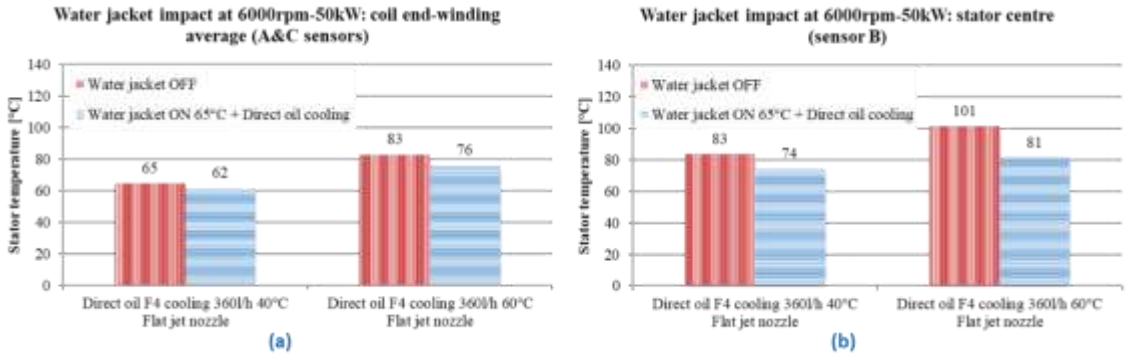

Figure 19 Water jacket impact at 6000 rpm - 50 kW: (a) coil end-winding average, (b) stator centre

Figure 19 illustrates tests carried out without a water chamber with a low viscosity fluid (oil F4) and an operating point of 6000 rpm – 50 kW. The results show that the injection of oil on the coil end-winding without the presence of the water chamber around the stator grid is sufficient to maintain the temperature in the engine below the reference value (see Figure 14) in continuous operation. The temperature gradient in the stator is higher for tests without water. Among the five sensors integrated in the winding, the temperature at the stator centre shows a highest increase when removing the water circuit. This is consistent with the cooling architecture: the oil is sprayed on both sides of the stator, so it has a more significant impact on the coil heads and moves the hot spots towards the centre. Also, at 40 °C, the thermal power absorbed by the oil is about 400 W

lower compared to a test with an active water jacket cooling. This confirms that the oil captures heat from the water in addition to that from the machine. Moreover, there is a lower variation in the power captured by the oil with temperature without the presence of the water chamber (for a passage of cooling from 40 °C to 60 °C, a variation of about 200 W without water against 1400 W with the presence of the water jacket).

The comparison of performance for indirect water jacket cooling and direct oil cooling could be conducted observing two physical quantities: thermal flow and stator temperature. Figure 20 illustrates the thermal flow absorbed by water and oil circuits, in a test where the two cooling systems are both active at an operating point of 6000 rpm – 50 kW. The temperature of water and oil is similar; however, oil begins to absorb more heat at a flow rate of 240 l/h, which is a third of the water flow rate of 720 l/h, and this trend increases with the oil flow rate. Figure 21 illustrates the stator temperature of the electric machine cooled by either water jacket or direct oil jet. It can be clearly observed that oil reduces significantly the coil end winding temperature by the direct contact. The stator centre temperature increases slightly with direct oil cooling. This is completely coherent with the fact that the stator centre is more distant from the oil impact zone. Globally, the efficiency of direct oil cooling is well demonstrated from these comparisons.

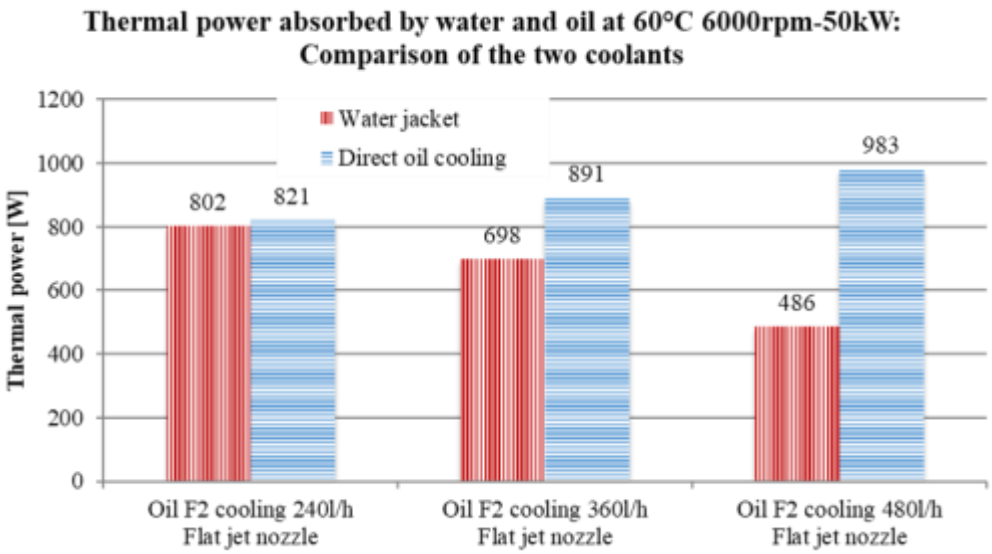

Figure 20 Comparison of thermal power absorbed by water and oil at 6000 rpm – 50 kW

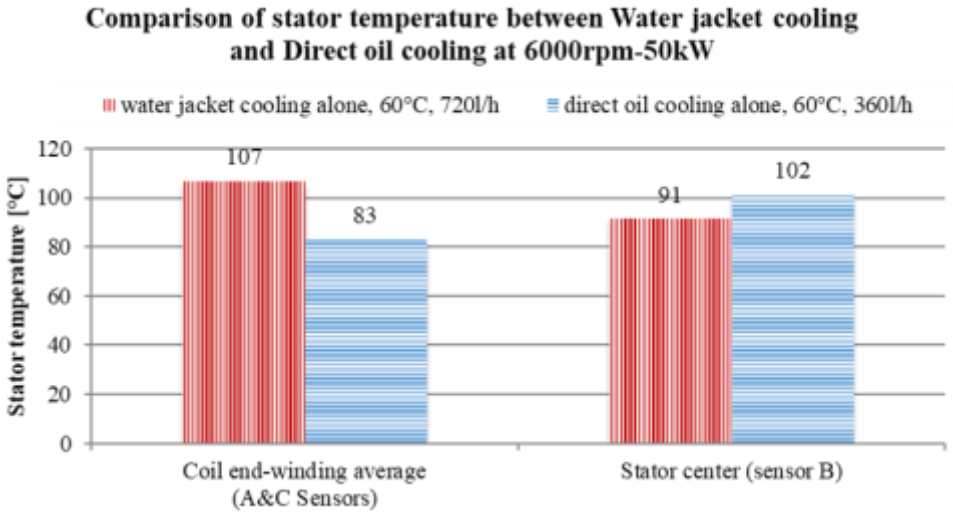

Figure 21 Comparison of stator temperature using water jacket cooling and direct oil cooling at 6000 rpm – 50 kW

In order to assess the aging of the fluids under direct operating conditions of the electric machine, samples are characterized at the start and at the end of each campaign dedicated to each fluid. The electrical resistivity and viscosity of the fluids are thus

measured. Among the four fluids in this study, the fluid referenced F1 exhibits the greatest change in electrical resistivity (at 90 °C, loss of approximately 34 MΩ.m between a new oil and an aged oil). This result is completely consistent because this fluid is used throughout the architecture discrimination campaign and therefore two to three times longer than the other three fluids. It should however be noted that the resistivity of the aged fluid is still appropriate for reuse in an electric motor. The viscosity of fluid F1 has increased slightly, this is also a sign of degradation. A *Fourier Transform InfraRed spectroscopy* analysis was conducted in order to determine the origin for this degradation. No significant peak increase is observed for the aged oil, which implies that the oil is not oxidized during the test. Elemental analysis show that the oil is not polluted by metal of the test rig. A possible explication for degradation is the pollution by water in the oil circuit or during the sample transport stage. For the two low viscosity fluids containing no polymers, the viscosity did not change significantly after the machine tests. The viscosity of fluid F4 slightly reduced after the campaign. This decrease in viscosity is explained by the degradation of the polymers present in this fluid. The fluid undergoes strong shearing in the injector, the polymer chains break, and the fluid permanently loses its viscosity [24]. However, after a rheological analysis carried out on this fluid before and after the tests, it is verified that the degradation of the polymers is not severe and retains its kinematic properties specific to the presence of polymers. This ensures that the polymer does not degrade severely in the injection devices.

As discussed in section 5.2, a repeatability and reproducibility campaign is carried out in this study to determine the degree of confidence in our various observations. This

campaign consists of repeating the same test several times. Five repetitions were performed for each test point. The test sequence is defined so that each repetition (for each point) is carried out on a different day and with the same initial conditions for starting the test (maceration time, mechanical stabilization of the machine, conditioning parameter of the fluid). Then, the methodology presented throughout this document is deployed for each test and the standard deviations are quantified to give the dispersion of the tests. Throughout this phase, a maximum standard deviation of 36 W (for thermal power absorbed in coolant) and 0.6 °C (for all measured stator temperatures) is obtained for the water jacket reference tests. About the tests with oils (in addition to water), a maximum standard deviation of 21 W and 0.4 °C. This applied for the entire operating range up to 14 000 rpm and powers up to 60 kW.

The perspectives of this study include extensive tests without water, using other injection methods (as direct cooling of the windings coupled with rotor hollow shaft cooling [21]), and the study of multifunction fluids (lubrication-cooling coupling).

In order to improve the methodology, other aspects which could impact the oil cooling of the electric machine will be studied: additional information could be provided implementing a method for the visualization of the flows [19, 20] to allow for a better understanding of the phenomena observed by measuring viscous friction losses. It is also planned to add more sensors in order to have a more accurate measurement of the stator temperature distribution, and for the monitoring of the bearing's temperature. The thermal insulation of the electric machine will also be enhanced with the use of a climatic chamber, to improve the quality criterion of the tests [8].

7. Conclusion

In this study, experimentations carried out aimed at understanding and characterizing the thermal behaviour of electric motors incorporating direct oil cooling are presented. A prototype representative of traction electric motors in terms of operating range is manufactured integrating different cooling architectures. A test bench capable of accommodating several types of oils is implemented. The instrumentation and the associated methodology are defined in order to assess the friction losses, the heat exchanges and the electric motor thermal behaviour.

Four fluids that are electrically compatible with motor active parts and have different properties are selected and prototyped by Total™. They are chosen by their chemistry and physicochemical properties in order to understand the impact of oils on cooling. The influence of the cooling architectures, flow rate, temperature on their performance is also assessed. Several configurations of oil cooling systems are thus evaluated at different operating points and different parametric variations.

Several campaigns are carried out in order to understand and evaluate the impact of different oils and architectures of direct cooling on the functions of the electrical machine. The test results make it possible to verify and quantify the gain on the thermal behaviour obtained by adding an oil injection system directly to the active parts of the machine (in addition to the indirect water-cooling system at the stator level). For example, a significant decrease of around 50°C in the coil end-winding temperature can be observed at an operating point of 6000 rpm - 50 kW. This gain is observed for various operating points and a variation of the oil cooling parameters. The observations and

results are confirmed by a repeatability and reproducibility study for speed values up to 14 000 rpm and continuous powers up to 60 kW.

A discrimination of the effect of the oil on cooling is also achieved, allowing to evaluate the impact of physico-chemical properties of oils on direct cooling performance as well as the impact of different cooling architectures selected for the study. The viscous friction losses are also observed in order to quantify the influence of the addition of oil on the active parts of the engine - due to the direct injection type, the parameters of the cooling (temperature, flow), or the chemistry and physicochemical properties of oils.

Further investigations will be carried out on a new version of the electric motor including direct injection supplied by the rotor shaft, and an enhanced instrumentation (oil injection visualization, sensors for an extended stator temperature distribution, bearings and rotor temperature monitoring) will be provided for a better understanding of the thermal issues. New multifunction fluids prototyped by Total™ will also be evaluated for the lubrication and cooling functions.

8. Nomenclature

α_{HTC}	heat transfer coefficient
Cp	specific heat capacity
ΔT_{x-y}	temperature gradient between *x* and *y*
F_h	Figure of Merit on average heat transfer
K	thermal conductivity

$\dot{m}$	mass flow
v	kinematic viscosity (*KV*)
P	thermal power
R_{th}	thermal resistance
ρ	Density
S_e	exchange surface
T	Temperature

9. Conflict of interest

The authors declare that there is no conflict of interest.

10. Acknowledgment

The authors gratefully acknowledge the contributions of the people from the IFPEN Mobility and Systems Research Division involved in this project. This study would not have been possible also without the collaboration with Total™.

11. References

[1] Davin, T., Pelle, J., Harmand, S., Yu, R., 2015, "Experimental study of oil cooling systems for electric motors," Appl. Therm. Eng., 75, pp. 1–13. DOI: 10.1016/j.applthermaleng.2014.10.060.

[2] Gai, Y., Kimiabeigi, M., Chuan Chong, Y., Widmer, J. D., Deng, X., Popescu, M., Steven, A., 2019, "Cooling of Automotive Traction Motors: Schemes, Examples, and Computation Methods," IEEE Transactions on Industrial Electronics, 66(3). DOI: 10.1109/tie.2018.2835397.

[3] Li, B., Kuo, H., Wang, X., et al., 2020, “Thermal Management of Electrified Propulsion System for Low-Carbon Vehicles,” Automot. Innov., 3, pp. 299–316. DOI: 10.1007/s42154-020-00124-y.

[4] Bertin, Y., 1999, "Refroidissement des machines électriques tournantes," Tech. Ing. D3460 v1.

[5] Bertin, Y., 2006, "Refroidissement des machines tournantes. Études paramétriques," Tech. Ing. D3462 v1.

[6] Gundabattini, E., Mystkowski, A., Idzkowski, A., R., R.S., Solomon, D.G., 2021, "Thermal Mapping of a High-Speed Electric Motor Used for Traction Applications and Analysis of Various Cooling Methods—A Review," Energies, 14(5), 1472. DOI: 10.3390/en14051472.

[7] Mock, P., 2019, “CO2 emission standards for passenger cars and light-commercial vehicles in the European Union,” last modified January 23, 2019, https://theicct.org/sites/default/files/publications/EU-LCV-CO2-2030_ICCTupdate_20190123.pdf.

[8] McLeod, P., Bradley, K.J., Ferrah, A., Magill, R., Clare, J.C., Wheeler, P., Sewell, P., 1998, “High precision calorimetry for the measurement of the efficiency of induction motors,” IEEE IAS, 1, pp. 304–311. DOI: 10.1109/IAS.1998.732311.

[9] Wang, R., Wang, Y., Feng, C., Zhang, X., 2015, “Powertrain preheating system of tracked hybrid electric vehicle in cold weather,” Appl. Therm. Eng., 91, pp. 252–258. DOI: 10.1016/j.applthermaleng.2015.08.027.

[10] He, H., Zhou, N., Sun, C., 2017, “Efficiency decrease estimation of a permanent magnet synchronous machine with demagnetization faults,” Energy Procedia, 105, pp. 2718–2724. DOI: 10.1016/j.egypro.2017.03.922.

[11] Park, M.H., Kim, S.C., 2019, “Thermal characteristics and effects of oil spray cooling on in-wheel motors in electric vehicles,” Appl. Therm. Eng., 152, pp. 582-593. DOI: 10.1016/j.applthermaleng.2019.02.119.

[12] Staton, D.A., Popescu, M., Hawkins, D., Boglietti, A., Cavagnino, A., 2010, “Influence of different end region cooling arrangements on end-winding heat transfer coefficients in electrical machines,” IEEE Energy Conversion Congress and Exposition, pp. 1298-1305. DOI: 10.1109/ECCE.2010.5617810.

[13] Kim, J., 2007, “Spray cooling heat transfer: The state of the art,” International Journal of Heat and Fluid Flow, 28(4), pp. 753-767. DOI: 10.1016/j.ijheatfluidflow.2006.09.003.

[14] Jafari, M., 2014, “Analysis of heat transfer in spray cooling systems using numerical simulations,” Electronic Theses and Dissertations, Paper 5028. http://scholar.uwindsor.ca/etd

[15] Ehrenpreis, C., El Bahi, H., Xu, H., et al., 2020, “Physically-motivated Figure of Merit (FOM) assessing the cooling performance of fluids suitable for the direct cooling of electrical components,” IEEE Intersociety Conference on Thermal and Thermomechanical Phenomena in Electronic Systems, pp. 422-429. DOI: 10.1109/ITherm45881.2020.9190343.

[16] Boglietti, A., Cavagnino, A., Staton, D., Shanel, M., Mueller, M., Mejuto, C., 2009, "Evolution and Modern Approaches for Thermal Analysis of Electrical Machines," IEEE Transactions on Industrial Electronics, 56(3), pp. 871-882. DOI: 10.1109/TIE.2008.2011622.

[17] Boglietti, A., Cossale, M., Popescu, M., Staton, D. A., 2019, "Electrical Machines Thermal Model: Advanced Calibration Techniques," IEEE Transactions on Industry Applications, 55(3), pp. 2620-2628. DOI: 10.1109/TIA.2019.2897264.

[18] Vanhaelst, R., Kheir, A., Czajka, J., 2016, “A systematic analysis of the friction losses on bearings of modern turbocharger,” Combustion Engines, 164(1), pp. 22-31. DOI: 10.19206/CE-116485.

[19] Liu, C., et al., 2020, “Experimental Investigation on Oil Spray Cooling With Hairpin Windings,” IEEE Transactions on Industrial Electronics, 67(9), pp. 7343-7353. DOI: 10.1109/TIE.2019.2942563.

[20] Ha, T., Kim, D. K., 2021, “Study of Injection Method for Maximizing Oil-Cooling Performance of Electric Vehicle Motor with Hairpin Winding,” Energies, 14, 747. DOI: 10.3390/en14030747.

[21] Lehmann, R., Petuchow, A., Moullion, M., Künzler, M., Windel, C., Gauterin, F., 2020, “Fluid Choice Based on Thermal Model and Performance Testing for Direct Cooled Electric Drive,” Energies, 13, 5867. DOI:10.3390/en13225867.

[22] Dairay, T., Fortuné, V., Lamballais, E., Brizzi, L., 2015, “Direct numerical simulation of a turbulent jet impinging on a heated wall,” Journal of Fluid Mechanics, 764, pp. 362-394. DOI: 10.1017/jfm.2014.715.

[23] Cornacchia, I., Pilla, G., Chareyron, B., Bruneaux, G., Kaiser, S., Poubeau, A., 2021, "Development of an Experimental Methodology to Characterize Liquid Cooling Systems for Electric Motors," IEEE International Electric Machines & Drives Conference, pp. 1-7. DOI: 10.1109/IEMDC47953.2021.9449572.

[24] Wood, L. G., 1950, “The change of viscosity of oils containing high polymers when subjected to high rates of shear,” Br. J. Appl. Phys., 1(8), 202.

Figure Captions List

Table Caption List